

# **Framboidal pyrite formation in the bottom sediments of the South Caspian Basin under conditions of hydrogen sulfide contamination**

*N. Kozina, L. Reykhard, O. Dara, V. Gordeev*

Shirshov Institute of Oceanology RAS, Russian Academy of Sciences, Moscow, Russia

**Abstract.** Structural features and distribution of framboidal pyrite were studied during lithological, mineralogical and geochemical studies of sediments in the South Caspian Basin. The lithological and geochemical parameters affecting the intensity of the formation of authigenic pyrite in sediments of the South Caspian Basin under conditions of hydrogen sulfide contamination were determined. According to X-ray diffraction (XRD), the content of pyrite in pelitic ooze reaches 4%. Microscopic studies have shown that pyrite formation occurs intensively in sediments with a high content of biogenic mineral components, such as opal diatom frustules and calcite plates of coccolithophores. Scanning electron microscopy (SEM) has demonstrated the presence of spherical pyrite framboids, as well as individual pyrite crystallites and their disordered clusters of various shapes.

---

This is the e-book version of the article, published in Russian Journal of Earth Sciences (doi:10.2205/2018ES000639). It is generated from the original source file using LaTeX's **ebook.cls** class.

The diameter of the framboids varies from 3 to 10 microns. Pyrite crystallites have subspherical, complicated polyhedral, prismatic, octahedral, pentagonal dodekahedron shapes. The crystallite sizes range from 0.5 to 3 microns. Based on geochemical data, there is no direct correlation between the intensity of pyrite formation and the high content of such components as Fe and  $C_{org}$  in bottom sediments. We assume that the formation of authigenic framboid pyrite in surface sediments (including the fluffy layer) is most likely due to the presence of hydrogen sulfide contamination in the near bottom water of the South Caspian Basin. Framboidal pyrite in the deeper layers (up to a depth of 35 cm) is the result of diagenetic processes that occur in accordance with the classical scheme of vertical zonality of diagenetic transformations in sediments.

## Introduction

Authigenic pyrite in bottom sediments of various basins is formed, as a rule, at the stage of early diagenesis. This mineral is a typical indicator of anoxic conditions [*Kholodov*, 2006; *Naumov*, 1989; *Strakhov*, 1960; *Yu-*

*dovich and Ketris*, 2011]. The advent of new precision methods of mineral study such as SEM and X-ray spectral analysis allowed to reveal unusual shapes of authigenic pyrite in sea and ocean sediments. It was found that authigenic pyrite is often represented by framboidal aggregates of submicron-sized crystals (crystallites) [*Astakhova*, 2007; *Berber'yan and Skripchenko*, 1996; *Kozina*, 2015; *Kozina and Reykhard*, 2018; *Lein*, 1979; *Love*, 1957; *Novichkova et al.*, 2017; *Pilskaln*, 1991; *Sawlowicz*, 2000; *Schallreuter*, 1984; *Reykhard*, 2014; *Reykhard et al.*, 2018a, 2018b].

Definition “Framboidal pyrite” (derives from the French word “la framboise” that means raspberry) has been firstly entered by G. V. Rust [*Rust*, 1935] to designate spherical aggregates (clusters), composed from small crystals (crystallites) of pyrite. Detailed study of framboidal pyrite in sedimentary rocks of different age and composition has revealed a different degree of geometric ordering of crystallites in structure of framboids. Framboids consist of poorly oriented crystallites of various sizes as well as of ordered idiomorphic crystallites [*Berber'an*, 1983; *Sawlowicz*, 2000; *Savelieva*, 2013]. These crystallites of various shapes (cubic, octahedral, pentagonal dodecahedron) can create the densest packing in framboids with a high degree of orderliness.

Biogenic (bacterial) origin of the framboidal pyrite in sedimentary rocks and bottom sediments means it was formed because of activity of sulfate-reducing bacteria under anoxic conditions [*Frankel and Blakemore*, 1991; *Love*, 1957]. As a rule, anoxic conditions exist in the bottom sediments of normally aerated basins, at a depth of more than 20–25 cm below the sediment-water interface, where the aerobic-anaerobic and anaerobic diagenesis zone is located [*Kholodov*, 2006]. Another situation is observed in basins under conditions of hydrogen sulfide contamination where mass formation of authigenic framboidal pyrite takes place already in a water column, and in ooze of the upper layer of bottom sediments. This phenomenon was observed in the Black Sea sediment [*Pilskaln*, 1991], and also in a suspended matter in the Cariaco Basin (Caribbean Sea) [*Li et al.*, 2011].

Thus, the appearance of authigenic framboidal pyrite in the mineral composition of sediments is an important genetic feature that allows to understand diagenetic changes in sediments, the behavior of various compounds of such chemical elements as iron and sulfur, which participate in the global biogeochemical cycle; also, it provides insight into processes of microbial activity [*Reykhard*, 2014].

The authors of this study have found framboidal pyrite in surface sediments in the South Caspian Basin [*Kozina*, 2015], which occupies almost the entire southern part of the Caspian Sea (Figure 1a).

From a geological viewpoint, the South Caspian Basin has a number of properties. Its maximum depth is 1025 m. The bottom of the basin is complicated by numerous mud volcanoes. There are shows of active hydrotherms along the eastern coast of the South Caspian [*Dobrovolsky*, 1969]. The properties of sedimentation in the South Caspian Basin are determined by their location in the arid climate zone [*Lisitzin and Lukashin*, 2015].

It is important to note that since 1930 the unstable presence of hydrogen sulfide was recorded in bottom waters in the Southern Caspian [*Ambrosimov et al.*, 2014; *Ivanov et al.*, 2013; *Sapozhnikov et al.*, 2007]. The first data on the presence of small concentration of hydrogen sulfide were recorded in 1933–1934 [*Bruevich*, 1937].

Complex studies of changes in the hydrochemical regime were carried out in 1958–1962. In the South Caspian Basin, in the near-bottom horizons of the water column, a sharp increase in the oxygen content and complete absence of hydrogen sulfide were observed

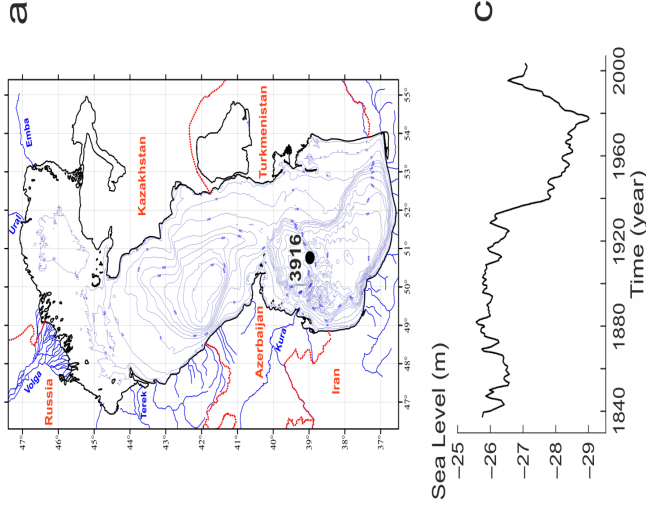


**Figure 1.** Research area, hydrophysical and hydrochemical characteristics of the Caspian Sea: a) – map-scheme of the research area and the location of the sampling Station 3916; b) – CTD-profiles of distribution of temperature ( $T$ ), salinity ( $S$ ), conventional density ( $\delta_t$ ), and oxygen ( $O_2$ ) in the water column of Station 3916 [Ivanov *et al.*, 2013]; c) – evolution of the level of the Caspian Sea in the 20th century in relation to the level of the World Ocean [Lebedev, 2005].

[*Ivanov et al.*, 2013]. Regular monitoring studies of the Caspian Sea were renewed by VNIRO scientist in 1995. In 2006, a sharp decrease in the oxygen content and the smell of hydrogen sulfide in the bottom waters of the South Caspian Basin were discovered [*Sapozhnikov et al.*, 2007]. In 2011, scientists of VNIRO discovered hydrogen sulfide in the near-bottom horizons of the water column (at a depth of 900 m) in the central part of the South Caspian Basin.

In 2012, detailed hydrological and microbiological studies revealed presence of dissolved hydrogen sulfide, occurrence of modern sulfate reduction processes, and the existence of anoxic regime under conditions of stable stratification at depths more than 880 m in the South Caspian Basin. The concentration of hydrogen sulfide increased from the upper bound of its detection layer to the bottom layers of the water column (from 60 to 240  $\mu\text{l L}^{-1}$ , respectively) (Figure 1b). Active processes of bacterial sulfate reduction were also recorded in the surface sediments (depth 0–1.5 cm) [*Ivanov et al.*, 2013]. Hydrogen sulfide contamination was observed against the background of significant sea level fluctuations (Figure 1c), which were associated with both climatic changes and the influence of the anthropogenic factor [*Ivanov et al.*, 2013].

Our research thoroughly studies framboidal pyrite in sediments of the South Caspian Basin in order to reveal structural characteristics of pyrite aggregates and the pattern of their distribution in sediments, as well as to reveal lithological and geochemical features of the authigenic pyrite formation process under conditions of hydrogen sulfide contamination in the Caspian Sea.

## Material and Methods

The studied material was sampled during the 39th cruise of the R/V *Rift* in 2012 within the framework of the project “The Caspian Sea System” under the guidance of Academician A. P. Lisitzin [*Ambrosimov et al.*, 2014; *Lisitzin*, 2016].

Sampling of sediments was carried out in the central part of the South Caspian Basin (Station 3916, 38°58.528' N, 50°45.738' E) (Figure 1a) at depth 1000 m by the multicorer “KUM” (Germany). The boundary layer between the water column and the condensed sediments, the so-called “fluffy layer”, is not disturbed during sampling by the multicorer.

Samples of sediments were taken from the core (35 cm in length and 10 cm in diameter) with different discretion ranged from 0.5 cm at the top of the column to

5.0 cm at the bottom of the column. The identification of lithological types of sediments was carried out according to the classification adopted in the Shirshov Institute of Oceanology, RAS [*Lisitzin*, 1986].

Mineralogical and geochemical studies of sediments were carried out in the Analytical Laboratory and in the Laboratory of Physical-Geological Research in the Shirshov Institute of Oceanology, RAS. An analysis of the mineral composition was carried out by means of a X-ray diffractometer D8 ADVANCE (Bruker AXC, Germany). Visualization of microcomponents of various genesis in sediments and determination of their elemental composition were carried out by means of scanning electron microscopy (SEM) using a scanning electron microscope SEM Vega 3 Tescan (TESCAN, Czech Republic) with a X-ray spectral microanalyzer INCA Energy (OXFORD Instruments, UK). The total iron content ( $Fe_{tot}$ ) in sediments was measured by the method of flame atomic absorption on the spectrophotometer "Kvant-2A" in the air-acetylene flame. The measuring of total, organic and carbonate carbon was carried out by coulometric titration by means of an AN-7529 carbon analyzer.

# Results

Lithological and geochemical analysis of sediments at St. 3916 showed that they are interbeddings of pelitic ooze with an insignificant content of a sandy and silty impurity, mainly slightly calcareous. The texture of ooze is microlayered and porous-cavernous. A high content of hydrotroilite inclusions, bundles and thin layers are present in sediments. Up to depth 8 cm there is a strong smell of hydrogen sulfide in sediments (Figure 2).

According to the data of microscopic studies and XRD, the mineral composition of sediments is mainly represented by quartz (14–29%), feldspars (albite up to 16%, potassium feldspar up to 15%) and clay minerals (illite up to 21%, kaolinite up to 8%, chlorite up to 14%, montmorillonite up to 0.5%) in different ratios.

Minerals of heavy fraction, such as amphiboles, pyroxenes, zircon, tourmaline, garnet, epidote, kyanite, apatite, ore minerals are present as accessory impurities. Shell detritus, coccoliths, opal frustules of diatoms, plant fragments are observed as inclusions [Kozina, 2017]. Also unusual biomorphic structures were found by the SEM method [Kozina et al., 2016].

A distinctive feature of studied sediments is high con-

Layer, №	Interval, cm		Thickness, cm
7	0-0.5		0.5
6	0.5-1.5		1.5
5	1.5-5.0		3.5
4	5.0-9.0		4
3	9.0-15.0		6
2	15.0-18.0		3
1	18.0-35.0		17



1



2



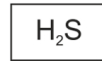
3



4



5



6



7



8

**Figure 2.** Lithological characteristics of bottom sediments of the South Caspian Basin (Station 3916): 1) – pelite with silty impurity; 2) – pelite with sandy and silty impurity; 3) – inclusion of hydrotroilite; 4) – hydrotroilite layers; 5) – porous-cavernous texture; 6) – hydrogen sulphide; 7) – distinct boundary; 8) – gradational contact.

*Layer 7.* Pelitic ooze with silty impurity, highly water-saturated (“fluffy-layer”), represented by flakes of black and greenish-gray color of 2–5 mm in size, with a strong smell of hydrogen sulfide.

*Layer 6.* Pelitic ooze with silty impurity, slightly calcareous, is greenish-brown in color with numerous inclusions of black hydrotroilite, with the smell of hydrogen sulfide.

*Layer 5.* Pelitic ooze with sandy and silty impurity, greenish-gray color. The degree of calcareousness varies from bottom to top along the section: from calcareous in the lower part of the layer to slightly calcareous at the upper contact. Spherical hydrotroilitic bundles with a diameter of not more than 1 mm are present at levels of 2.5, 3.5 and 4.5 cm. There is a smell of hydrogen sulfide.

*Layer 4.* Pelitic ooze with silty impurity, calcareous, grayish-green color. The texture is micro-layered in the form of a clear interlayering of layers of pelitic ooze grayish-green (2 mm thick) and black hydrotroilite layers (1 mm thick). In the interval from 5 to 8 cm there is a smell of hydrogen sulfide.

*Layer 3.* Pelitic ooze with sandy and silty impurity, slightly calcareous to calcareous, light gray. Hydrotroilite microlayers are in the interval of 11–12 cm. Caverns of irregular or rounded shape no larger than 5 mm appear in the interval of 11–15 cm.

*Layer 2.* Pelitic ooze with silty impurity, slightly calcareous, gray. The texture is micro-layered in the form of a clear interlayering of thin layers of gray pelitic ooze (up to 2 mm thick) and black hydrotroilite layers (up to 1 mm thick). There are pores and caverns.

*Layer 1.* Pelitic ooze with sandy and silty impurity, calcareous in the lower part of the layer, slightly calcareous in the upper part of the layer, light gray, chalk-like color, with black hydrotroilite inclusions. Spherical hydrotroilite bundles with a diameter of less than 1 mm are in the interval of 19–20 cm. The texture is porous-cavernous.

tents of authigenic sulfate and carbonate minerals, such as gypsum (up to 25%), calcite (up to 8%), magnesian calcite (up to 11%), kutnahorite (up to 6%) [*Dara et al.*, 2015; *Kozina*, 2017]. High concentration of halite has been recorded at the top of the column (16% in the interval 0–0.5 cm).

XRD analysis of sediments at St. 3916 revealed insignificant content of pyrite. It was less than 4%. Its maximal concentration has been registered in the interval 6–7 cm. According to SEM, in pelitic ooze at St. 3916 pyrite is present as framboids and crystallites (Figure 3, Figure 4). Disordered crystallite clusters are most likely the results of mechanical destruction of the framboids.

Framboidal pyrite is formed on the plant fragments, on the diatom frustules (Figure 3a, Figure 4f) and in the pore intergranular space of sediments (Figure 3b). In pelitic ooze, there are single framboids and their clusters, where each framboid is represented as an isolated individual aggregate of crystallites. The sizes of framboids vary ranging from 3 up to 10  $\mu\text{m}$  in diameter.

Generally, framboids have the low degree of ordering, which slightly changes from top to down in the column. Geometrically disordered framboids are located in the upper part of the column (Figure 3c). They consist

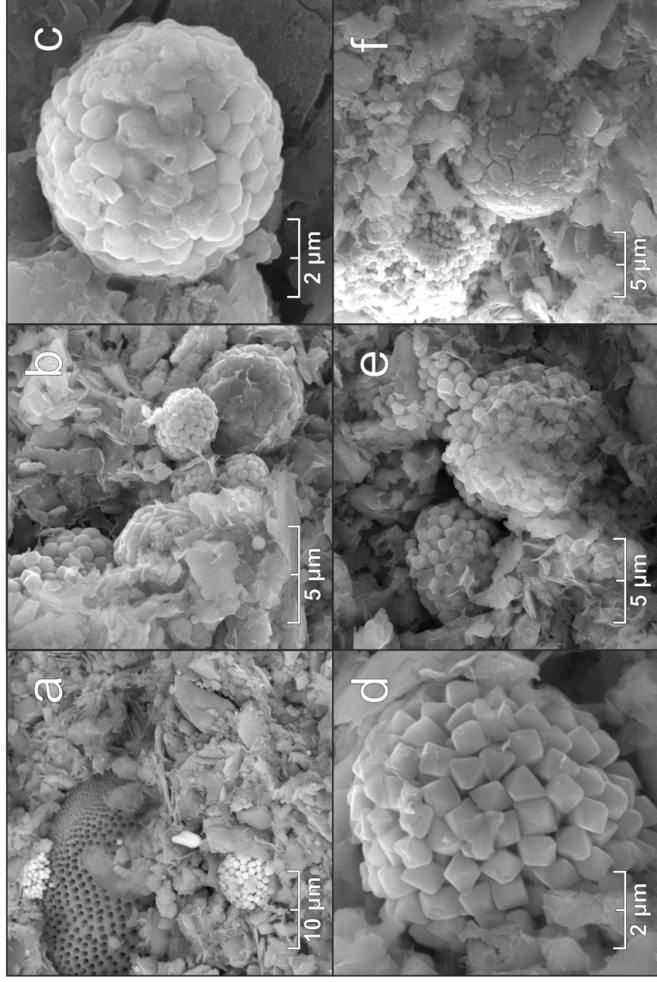


**Figure 3.** Framboids of pyrite in the bottom sediments of the South Caspian Basin: a) – pyrite framboids and crystallites on the diatom frustules; b) – pyrite framboids in the pores of pelitic ooze; c) – geometrically disordered framboids from crystallites of various sizes and shapes; d) – framboids with low degree of ordering of octahedral crystallites; e) – crystallites with a corroded surface; f) – framboid with desiccation cracks.

of randomly distributed crystallites of different shapes. Faintly discernible orientation and sizing of octahedral crystallites in framboids with low degree of ordering has been noted in bottom intervals (Figure 3d).

Pyrite crystallites of subspherical, complicated polyhedral (Figure 4a), prismatic (Figure 4b), octahedral (Figure 4c), pentagonal dodekahedron shapes were observed. Besides, intensively corroded crystallites were found in the top part of the column (Figure 4d) while strong deformation of crystallites have been recorded in low part of the column (Figure 4e). Sizes of crystallites are from 0.5 to 3  $\mu\text{m}$ .

Thus, the general distinctive feature of studied pyrite aggregates is structural imperfection such as poor sorting of crystallites in shape and sizing, low degree of geometrical ordering of crystallites and density of their packing in the volume of framboids, corroded surface of crystallites (Figure 3d), deformation of crystallites and framboids. Sometimes we registered cracks, which looked like desiccation cracks (syneresis?) in framboids (Figure 3f).

Geochemical researches showed that studied sediment of the South Caspian Basin was highly but unevenly enriched with a calcium carbonate (Figure 2), organic matter, and iron. Content of sulfur in sedi-

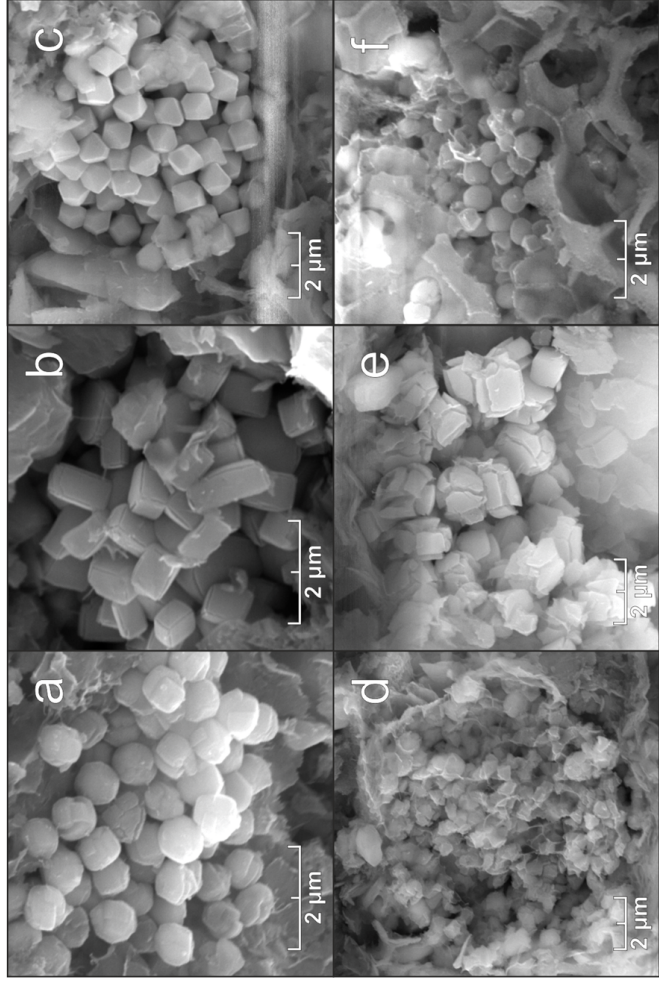


**Figure 4.** Pyrite crystallites in the bottom sediments of the South Caspian Basin: a) – polygonal crystallites of complicated shape with deformation features; b) – prismatic crystallites; c) – octahedral crystallites; d) – intensively corroded crystallites; e) – severely deformed crystallites; f) – pyrite crystallites on detritus of diatoms frustules.

ments at St. 3916 wasn't measured at this stage of the study.

Content of iron ( $Fe_{tot}$ ) strongly varies ranging from 1.2% up to 6.6% along the column without visible regularity. Content of  $Fe_{tot}$  from 2.8% (in the interval of 0–0.5 cm) up to 6.6% (in the interval of 9–10 cm) was registered in layers where XRD showed the content of pyrite more than 1%. The maximal content of pyrite was measured in the interval of 6–7 cm where content of  $Fe_{tot}$  was just 4.4%.

Results of organic carbon ( $C_{org}$ ) measuring in the sediment column at St. 3916 showed that the top layers were highly enriched with  $C_{org}$ . Content of  $C_{org}$  reached the maximum (8.7%) in a fluffy layer [*Lein et al.*, 2014]. Down the column,  $C_{org}$  unevenly decreased to minimum (1.47%) in the interval of 24–26 cm. In intervals of intensive pyrite formation, content of  $C_{org}$  fluctuated from 1.75% (interval of 33–35 cm, where quite high content of pyrite was (3%)) to 8.7% (in a fluffy layer, where the content of pyrite was just 1%). Maximal content of pyrite corresponds to a high content of organic carbon ( $C_{org}$  2.24%).

Thus, we can conclude that there is no direct correlation between the highest concentrations of iron, organic matter and maximal content of pyrite in the studied

sediments. At the same time, it is obvious that the formation of established contents of pyrite (1–4%) required heightened concentrations of Fe ( $\geq 2.8\%$ ) and  $C_{\text{org}}$  ( $\geq 1.75\%$ ).

A high content of gypsum is an indirect sign of high concentrations of sulfur in the sediments of St. 3916. In particular, the content of gypsum in a fluffy layer reaches 7% while it is 22–25% in the interval 0.5–1.5 cm. Below the column, contents of gypsum falls abruptly to 3% (in interval of 2.5–3.0 cm). It fluctuates within 0–3% along whole column of sediments, raising up to 8% just in the interval 33–35 cm. It is important that, according to XRD and SEM data, pyrite was not detected in the bottom sediments with the maximum content of gypsum. On the contrary, the maximum content of pyrite has been recorded in sediments included only 2% of gypsum.

## Discussion

The complex studies have revealed framboidal pyrite as one of the most widely occurring authigenic minerals in modern sediments in the South Caspian Basin. The presence of pyrite in sediments is associated with the specific geological, hydrological and geochemical

conditions of this area.

Firstly, these are specific hydrological conditions in the deep-water stagnant closed basin in the arid zone. They contributed to the accumulation of thickness of pelitic ooze, enriched with organic matter, iron, sulfates and carbonates.

Secondly, the presence of high concentrations of hydrogen sulfide in the near bottom layers of the water column and in bottom sediments in the South Caspian Basin [*Lein et al.*, 2014] means there are reducing conditions in the upper layer of bottom sediments.

It is expected that the total amount of pyrite that can form in sediments at the stage of early diagenesis is limited by sedimentation rate of decomposable organic matter, dissolved sulfate and iron minerals [*Savel'eva*, 2013]. It is known, the abundance of organic matter in the sediment makes it possible to develop sulfate-reducing bacteria. These bacteria reduce the sulfate of seawater and release hydrogen sulfide reacting with the labile iron, which ultimately leads to the formation of pyrite [*Volkov*, 1979].

As it was shown above, the content of  $C_{org}$  in bottom sediments in the South Caspian Basin is very high, especially in a surface layer. This creates favorable conditions for life of microorganisms, the total number of

which is 150/180 106 cells  $\text{cm}^{-3}$  in the fluffy layer, and 1500/1800 cells  $\text{cm}^{-3}$  in the interval of 0.5–1.5 cm [*Lein et al.*, 2014]. Iron enters in the sea among the contents of terrigenous runoff from the catchment area, partly with eolian material and, possibly, with the hydrothermal waters of Cheleken [*Lukashin and Lisitzin*, 2016; *Lukashin et al.*, 2016]. The probability of high sulfate content in the pore waters was noted earlier. All the components entering the South Caspian Basin are accumulated in sediments as a result of the climate aridity and the absence of outflow from the Caspian Sea.

This combination of environmental factors leads to the appearance of small amount of pyrite which is already present in the fluffy layer. Part of the pyrite in the fluffy layer and in the deep layers of the column can be the product of erosion of ancient pyrite-containing sediments or the product of underwater mud volcanoes [*Lebedev et al.*, 1973; *Kholodov et al.*, 1989]. Nevertheless, the formation of framboidal pyrite in the fluffy layer is also possible. Our studies have established all the necessary components and conditions for pyrite formation in this interval.

The maximal concentration of pyrite in the interval of 6–7 cm is most likely the result of physical and

chemical processes of reductive diagenesis. Probably at this depth a phased mechanism of pyrite formation is realized through the bacterial reduction of colloidal hydrotroilite [*Butler and Rickard*, 2000; *Vaughan and Corckhill*, 2017], which is the primary form of authigenic sulfide [*Frolov*, 1992; *Strakhov*, 1960]. At this interval, hydrotroilite is represented by well-defined layers with a thickness of 1 mm (Figure 2).

Down the column, the pyrite concentration changes insignificantly (from 1 to 3%). The smell of hydrogen sulfide disappears at a depth of 8 cm. But the high porosity of the sediments in the lower part of the column (up to 35 cm), noted directly during sampling, indicates their strong gas saturation. This can indirectly indicate current active microbial processes. High  $Fe_{tot}$  and  $C_{org}$  contents are fixed along the whole length of the column. The hydrotroilite disappears at a depth of 20 cm (Figure 2). According to SEM data, sulfidization in the interval 20–35 cm is represented only in the form of pointwise pyritization of different intensity. This is confirmed by the results of X-ray phase analysis.

# Conclusion

At this stage of the study, we detected some features of the formation of authigenic pyrite in the bottom sediments of the South Caspian Basin.

The formation of authigenic pyrite was found in surface sediments (including the fluffy layer) [*Kozina*, 2015]. This is most likely due to the presence of hydrogen sulfide contamination in the near-bottom water column in the Southern Caspian Basin. Framboidal pyrite on deeper layers (to a depth of 35 cm) is the result of processes of reductive diagenesis in accordance with the classical scheme of diagenetic transformations in sediments.

The maximum pyrite content (4%) was measured in the sediment layer (7–8 cm interval) with high (but not maximal!) concentrations of  $Fe_{tot}$  and  $C_{org}$ . In our opinion, this fact indicates the absence of a direct correlation between the intensity of pyrite formation and the contents of only these components in bottom sediments.

The studied pyrite framboids are mainly characterized by a low degree of geometric ordering, which may be a consequence of the incompleteness of pyrite crystallization process.

Corrosivity and deformation of crystallites and framboids, most likely, arose in conditions of an aggressive physical and chemical environment. They can also be associated with processes of densification and dehydration of sediments during diagenetic transformations.

In the deepest region of the South Caspian Basin the formation of pyrite occurs in pelitic ooze with highly mineralized porous waters, as evidenced by the high content of authigenic carbonate and sulfate minerals in the sediments [*Kozina*, 2017].

Pyrite formation intensively occurs in pelitic sediments saturated with biogenic mineral components (opal detritus of diatoms and calcite plates of coccolithophores). In these deposits, we recorded a very high content of  $C_{org}$ . Probably, these facts indicate that in the process of pyrite formation a bacterial transformation of an organic matter predominantly of planktonogenic genesis occurs.

Thus, we established the absence of a direct correlation between the high content of some components necessary for the formation of pyrite in bottom sediments, and the actual maximum concentrations of pyrite. This indicates the need to identify other factors that control the formation of framboidal pyrite in sediments in the South Caspian Basin.

**Acknowledgments.** The authors are grateful to A. K. Ambrosimov, A. A. Klyuvitkin, M. D. Kravchishina, N. V. Politova, A. N. Novigatsky for assistance in the cruise, and V. A. Karlov, L. V. Demina, A. N. Rudakova for analytical tests. The authors also thank Academician A. P. Lisitzin and Dr. A. Yu. Lein for helpful discussions and advice providing. Preparation and processing of samples was carried out with the support of the grant RSF # 14-27-00114. The results of studies of bottom sediments of the Caspian Sea were obtained within the RFBR grant (project # 16-35-60028). The results of analysis of hydrological data were obtained in the framework of the state assignment of FASO Russia (theme # 0149-2019-0004.)

## References

- Ambrosimov, A. K., et al. (2014), Multidisciplinary studies of the Caspian Sea system during cruise 39 of the R/V Rift, *Oceanology*, 54, no. 3, p. 395–399.
- Astakhova, N. V. (2007), *Authigenic Formations in the Late Cainozoic Deposits of the Boreal Seas of East Asia*, 244 pp., Dal'nauka, Vladivostok.
- Berber'yan, T. K. (1983), Framboid-pyrite aggregates in ores of pyrite deposits and their genetic and search value, Dissertation of the candidate of geological and mineralogical sciences, Novocherkassk Polytechnic Institute S. Ordzhonikidze, Novo-

cherkassk.

Berber'yan, T. K., N. S. Skripchenko (1996), *Structure of the Framboidal Pyrite of the Modern Silt in the Black Sea*, 62–65 pp., Novocherkassk Polytechnic Institute S. Ordzhonikidze, Novocherkassk.

Bruevich, S. V. (1937), *Hydrochemistry in the Middle and Southern Caspian*, 352 pp., AS USSR, Moscow.

Butler, I. B., D. Rickard (2000), Framboidal pyrite formation via the oxidation of iron (II) monosulphide by hydrogen sulphide, *Geochim. Cosmochim. Acta*, 64, no. 15, p. 2665–2672,

### **Crossref**

Dara, O. M., A. Y. Lein, N. V. Kozina, M. V. Ivanov (2015), First find of kutnohorite in modern sediments of the Caspian basin, *Doklady Earth Sciences*, 465, no. 2, p. 1257–1261.

Dobrovolsky, A. D. Ed. (1969), *Caspian Sea, Issue 1*, 264 pp., MSU Press, Moscow.

Frankel, R. B., R. P. Blakemore eds. (1991), *Iron Biominerals: An Overview. Iron Biominerals*, 435 pp., Plenum Press, New York,

### **Crossref**

Frolov, V. T. (1992), *Lithology, Educational book, 1*, 336 pp., MSU, Moscow.

Ivanov, M. V., A. S. Savvichev, A. A. Klyuvitkin, E. E. Zakharova, I. I. Rusanov, A. Yu. Lein, A. P. Lisitzin, A. L. Chul'tsova (2013), Resumption of hydrogen sulfide contamination of the water column of deep basin in the Caspian Sea, *Doklady Earth Sciences*, 453, no. 1, p. 1094–1099.

Kholodov, V. N. Eds., et al. (1989), *The Caspian Sea: Problems*

- of *Sedimentogenesis*, 184 pp., Nauka, Moscow.
- Kholodov, V. N. (2006), *Geochemistry of the Sedimentary Process, Proceedings of the Geological Institute of RAS*, 608 pp., GEOS, Moscow.
- Kozina, N. V. (2015), Mineral composition of bottom sediments and peculiarities of modern sedimentation in the Caspian Sea, Abstract of the candidate of geological and mineralogical sciences, IO RAS, Moscow.
- Kozina, N. V. (2017), Carbonate accumulation in the southern part of the Caspian Sea. Types and distribution in time, *Materials of the XXII International Scientific Conference (School) on Marine Geology*, 3, p. 315–320, IO RAS, Moscow.
- Kozina, N. V., L. Ye. Reykhard (2018), Formation of framboidal pyrite in bottom sediments of South Caspian Basin under conditions of hydrogen sulfide contamination, *Processes in Geomedia*, 17, p. 161–162.
- Kozina, N. V., A. Yu. Lein, O. M. Dara (2016), Unknown biomorphic structures – environmental formations or laboratory artifact?, *Priroda*, no. 4, p. 70–73.
- Lebedev, S. A., A. G. Kostianoy (2005), *Satellite Altimetry of the Caspian Sea*, 366 pp., Publishing Center OCEAN of the International Ocean Institute, Moscow.
- Lebedev, L. I., E. G. Maev, O. K. Bordovskaya, L. S. Kulakov (1973), *Osadki Kaspiyskogo Morya*, 119 pp., Nauka, Moscow (in Russian).
- Lein, A. Yu. (1979), Morphology and structure of pyrite and other sulfide minerals, *Lithology and Geochemistry of Bottom Sediments of the Pacific (Trans-oceanic Profile)*, p. 76–84,

Nauka, Moscow.

- Lein, A. Yu., et al. (2014), Microbiological and biogeochemical properties of the Caspian Sea sediments and water column, *Microbiology*, 83, no. 5, p. 648–660.
- Li, X., et al. (2011), Particulate sulfur species in the water column of the Cariaco Basin, *Geochim. Cosmochim. Acta*, 75, no. 1, p. 148–163, **Crossref**
- Lisitzin, A. P. (1986), Questions of marine geological mapping (on the example of the continental margin of Africa), *UNESCO Reports on Marine Sciences, No. 37*, p. 91, UNESCO, Paris.
- Lisitzin, A. P., V. N. Lukashin (2015), Composition of dispersed sedimentary matter and fluxes in the water column of the Caspian Sea, *Doklady Earth Sciences*, 464, no. 1, p. 956–962.
- Lisitzin, A. P. Ed. (2016), *The Caspian Sea System*, 480 pp., Scientific World, Moscow.
- Love, L. G. (1957), Micro-Organisms and the Presence of Syngenetic Pyrite, *Quart. J. Geol. Soc. London*, 113, p. 429–440.
- Lukashin, V. N., A. P. Lisitzin (2016), Geochemistry of dispersed sedimentary matter and its fluxes in the water column Caspian Sea, *Oceanology*, 56, no. 5, p. 675–689.
- Lukashin, V. N., A. P. Lisitzin, O. M. Dara, N. V. Kozina, A. A. Klyuvitkin, A. N. Novigatsky (2016), Mineral composition of sedimentary matter in the Caspian Sea, *Oceanology*, 6, no. 6, p. 852–862.
- Naumov, V. N. (1989), *Optical Component Determination of Sedimentary Rocks*, 347 pp., Nedra, Moscow.
- Novichkova, Ye. A., L. Ye. Reykhard, A. P. Lisitzin, A. Ye. Rybalko, A. de Vernal (2017), New data on the Holocene evolution

- of the Dvina Bay (White Sea), *Doklady Earth Science*, 474, Part 1, p. 607–611.
- Pilskaln, C. H. (1991), Biogenic aggregate sedimentation in the Black Sea basin, *Black Sea Oceanography*, Izdar E., Murray J. W. (eds.), p. 293–306, Kluwer, Dordrecht.
- Reykhard, L. E. (2014), Pyrite framboid in bottom sediments of the White Sea, *Materials of the Annual Meeting of the Russian Mineralogical Society*, p. 62–64, RMS, SPb.
- Reykhard, L. Ye., N. V. Kozina, Ph. V. Sapozhnikov, O. Yu. Kalinina (2018a), Framboidal pyrite: extreme biomineralization from the Arctic to the Antarctic, *Materials of VI International Symposium "Biog-enic-abiogenic interactions in natural and anthropoge-nic systems"*, p. 173–175, VVM publishing Lld, St. Petersburg.
- Reykhard, L., et al. (2018b), Biomineral indicators of hydrological, geological and climatic processes in the Arctic, *Acta Cryst.*, A74, p. e250.
- Rust, G. W. (1935), Colloidal primary copper ores at Cornwall mines southeastern Missouri, *J. Geol.*, 43, no. 4, p. 398.
- Sapozhnikov, V.V., O. K. Grashchenkova, K.K. Kivva, A. V. Azarenko (2007), Hydrological and hydrochemical studies of the middle and south Caspian Sea from the R/V Issledovatel' Kaspia (September 2–17, 2006), *Oceanology*, 47, no. 2, p. 290–293.
- Savel'eva, O. L., D. P. Savel'ev, V. M. Chubarov (2013), Pyrite framboids in carbonaceous rocks of the Smagin association of the Kamchatsky Cape peninsula, *Vestnik Kraunts. Earth Sciences*, no. 2, Issue 22, p. 144–151.
- Sawlowicz, Z. (2000), *Framboids: From Their Origin to Appli-*

- cation, 80 pp., Polska Akademia Nauk, Prace Mineralogiczne, Warsaw, Poland.
- Schallreuter, R. (1984), Framboidal pyrite in deep-sea sediments, *Initial Reports of the Deep Sea Drilling Project*, 75, p. 875–891.
- Strakhov, N. M. (1960), *Foundations of the Theory of Lithogenesis. Vol. II. Regularities of Composition and Distribution of Humid Sediments*, 574 pp., AS USSR, Moscow.
- Vaughan, D. J., C. L. Corkhill (2017), Mineralogy of sulfides, *Elements*, 13, no. 2, p. 81–87.
- Volkov, I. I. Ed. (1979), *Ocean Chemistry, Vol. 2*, 536 pp., Nauka, Moscow.
- Yudovich, Ya. E., M. P. Ketris (2011), *Geochemical Indicators of Lithogenesis*, 742 pp., Geoprint, Syktyvkar.
-